Transient diffusion and thermal processes in a finite one-dimensional harmonic crystal

Article *in* Journal of Physics Condensed Matter · October 2021

DOI: 10.1088/1361-648X/ac33dc

3 authors, including:

Andrey Murachev
Saint Petersburg State University
8 PUBLICATIONS **24** CITATIONS
SEE PROFILE

Denis Tsvetkov
Peter the Great St.Petersburg Polytechnic University
13 PUBLICATIONS **99** CITATIONS
SEE PROFILE

Transient diffusion and thermal processes in a finite one-dimensional harmonic crystal

A.M. Krivtsov,* A.S. Murachev,† and D.V. Tsvetkov
Department of Theoretical Mechanics, Peter the Great St. Petersburg Polytechnic University

In this paper, an instant homogeneous thermal perturbation in the periodic one-dimensional harmonic crystal is studied. The exact solution for thermal and diffusive characteristics is obtained, namely, particle velocity dispersion (kinetic temperature) and particle displacement dispersion. It is found that thermal and diffusion processes demonstrate a quasi-periodic recurrence. The recurrence interval is equal to the time it takes the sound wave to travel the half-length of the crystal. The "thermal echo" (sharp peaks in kinetic temperature) occurs in the system with the specified periodicity. Diffusion characteristics reveal large-scale time changes with a nearly complete return to the initial state at each quasi-period. It is also shown that the spatial mean squared displacements of particles are significantly different from the ensemble mean squared displacements.

I. INTRODUCTION

It is a difficult problem to develop an exact analytical model of non-stationary thermal and diffusion processes observed at the molecular level. So far, it has been done only for a limited group of systems. Considerable progress has been achieved for harmonic crystals [1–6] with linearized atomic interaction forces. Such an approximation is justified if the temperatures are far from melting points and the electronic subsystem does not significantly contribute to the overall dynamics of the crystal lattice. These conditions are naturally satisfied for covalent crystals. In the present paper, we analyze non-stationary thermo-diffusion processes in finite systems on the example of a one-dimensional harmonic crystal. Thermal processes are those involving random velocities of crystal particles and diffusion processes involve random displacements.

There are two types of thermal processes in crystals: fast and slow [6]. Fast processes are transient and are associated with energy redistribution between degrees of freedom, and slow processes are associated with heat transfer. In this paper, we will focus on fast processes only, so that the system state can be regarded as spatially uniform. Current technologies used to generate and measure ultra-short laser impulses [7–9] will make experimental studies of such processes possible in the near future. Additionally to thermal processes, the related diffusion processes are considered. No changes of particle order occur in a harmonic crystal, so the diffusion as particle mixing does not exist. However, a particle can move away to significant distances from its initial position as a result of thermal motion, so the corresponding diffusion processes are rather complicated and differ significantly from thermal processes. In particular, as we will show later, both fast and slow processes are realized for diffusion in the spatially uniform case. The study of systems containing a finite number of atoms [10–14] becomes especially relevant with nanotechnology development. Thermo-diffusion processes in such systems have several specific features related to their finite nature. In particular, the paper will demonstrate that fast thermal processes in the finite crystal periodically spontaneously recur. That is called the "thermal echo". Because of the slow diffusion processes the system returns to its initial state in time with an order of magnitude of the sound wave passing the crystal.

II. THE MODEL

One-dimensional crystals (chains) provide a convenient model to study thermomechanical processes in solids analytically [1, 15–19]. The equation of motion of one-dimensional harmonic crystal particles in the simplest case is

$$\ddot{u}_k = \omega_e^2 \left(u_{k-1} - 2u_k + u_{k+1} \right), \tag{1}$$

where $\omega_e \stackrel{\text{def}}{=} \sqrt{C/m}$ is the elementary frequency, m is the particle mass, C is the stiffness of interparticle spring, u_k is the displacement of the kth particle. Periodic boundary conditions are used for equation (1):

$$u_{k+N} = u_k, \tag{2}$$

where N is the number of particles in the crystal. Condition (2) might be interpreted as a one-dimensional crystal closed in a circle (Born-von Karman boundary condition [20]). We use thermal shock conditions as the initial condition:

$$t = 0: \qquad u_k = 0\,, \qquad \dot{u}_k = \sigma \rho_k, \tag{3}$$

where ρ_k are independent random numbers, σ is the initial velocity dispersion. For the random numbers ρ_k we have:

$$\rho_{k+N} = \rho_k\,, \qquad \langle \rho_k \rangle = 0\,, \qquad \langle \rho_k \rho_{k+n} \rangle = \delta_n^N. \tag{4}$$

Here and below angle brackets stand for mathematical expectation, $\delta_n^N = 1$ when n is divisible by N and $\delta_n^N = 0$ otherwise. Formulae (4) imply that the random variables are periodic in n, have zero mathematical expectation

* akrivtsov@bk.ru
† andrey.murachev@gmail.com

and unit dispersion, and they are independent if the indexes differ by less than N (in other words, there are N independent random variables).

Due to the linearity of the system (1), the displacements and velocities have zero mathematical expectations:

$$\langle u_k \rangle = 0\,, \qquad \langle v_k \rangle = 0, \tag{5}$$

where $v_k \stackrel{\text{def}}{=} \dot{u}_k$. Let us denote:

$$\overline{u} \stackrel{\text{def}}{=} \frac{1}{N}\sum_{k=1}^{N} u_k\,, \qquad \overline{v} \stackrel{\text{def}}{=} \frac{1}{N}\sum_{k=1}^{N} v_n \tag{6}$$

the spatial averages of particle displacements and velocities (hereafter, the dash above denotes the spatial average). Quantities (6) do not depend on k and are the velocity and displacement of the system's center of mass. For finite N, these quantities, unlike the mathematical expectations (5), are random and, generally speaking, nonzero. Only at $N \to \infty$ do the averages (6) tend to zero. This is the main difference between finite and infinite crystals.

Let us introduce centered displacements and velocities

$$\tilde{u}_k \stackrel{\text{def}}{=} u_k - \overline{u}\,, \qquad \tilde{v}_k \stackrel{\text{def}}{=} v_k - \overline{v}. \tag{7}$$

Unlike u_k and v_k, these quantities are materially objective, i. e., they do not change when the system's center of mass moves. Diffusion and thermal processes are defined, respectively, by centered displacement and velocity dispersions:

$$\langle \tilde{u}_k^2 \rangle\,, \qquad \langle \tilde{v}_k^2 \rangle. \tag{8}$$

In particular, the kinetic temperature of a one-dimensional crystal is

$$k_B T = m\langle \tilde{v}_k^2 \rangle, \tag{9}$$

where k_B is the Boltzmann constant. According to the problem statement, the values (8)–(9) depend on time but do not depend on the spatial index k.

Non-stationary processes are described using a method based on correlation analysis [1, 3, 4, 6, 21, 22]. Correlation analysis considers deterministic equations for statistical motion characteristics, i.e., covariances of particle displacements and velocities. These equations are closed-formed and allow one to obtain an analytical solution that includes, among other things, the dispersion (8) time function.

III. CORRELATION ANALYSIS

Let us consider the covariances of displacements and velocities:

$$\xi_n \stackrel{\text{def}}{=} \langle u_k u_{k+n} \rangle\,, \qquad \kappa_n \stackrel{\text{def}}{=} \langle v_k v_{k+n} \rangle. \tag{10}$$

Since the problem is spatially uniform, the covariances are independent of the index k, and depend only on the index n, which determines the distance between the correlating particles. Periodicity conditions (2) produce equivalent periodicity conditions for the covariances:

$$\xi_{n+N} = \xi_n\,, \qquad \kappa_{n+N} = \kappa_n. \tag{11}$$

The covariances differentiation considering the chain dynamics equation (1) leads to a closed system of dynamics equations for covariance. The simplest form can be obtained using an additional variable

$$\lambda_n \stackrel{\text{def}}{=} \kappa_n + \omega_e^2\,(\xi_{n-1} - 2\xi_n + \xi_{n+1})\,. \tag{12}$$

Then the following IVP (initial value problem) is a consequence of problem (1)–(3) [3, 22]:

$$\ddot{\lambda}_n = 4\omega_e^2\,(\lambda_{n-1} - 2\lambda_n + \lambda_{n+1})\,, \tag{13}$$

$$t = 0: \qquad \lambda_n = \sigma^2 \delta_n^N\,, \qquad \dot{\lambda}_n = 0. \tag{14}$$

This problem is equivalent to the IVP for a one-dimensional crystal (1), with one particle displaced at the initial moment and the rest being stationary. The important difference between the initial value problem (13)–(14) and the original IVP (1)–(3) is that it describes the dynamics of deterministic quantities λ_n, while the original IVP describes the dynamics of stochastic quantities u_k. The main difference comes from the initial conditions: in problem (13)–(14), they are deterministic, while in problem (1)–(3) the initial conditions are stochastic.

Given the periodic boundary conditions (11), problem (13)–(14) can be solved as the initial value problem for the system of N linear differential equations, which gives

$$\begin{aligned} &\lambda_n = \frac{\sigma^2}{N}\sum_{k=0}^{N-1} \cos q_k n \cos 2\omega_k t\,, \\ &q_k \stackrel{\text{def}}{=} \frac{2\pi k}{N}\,, \qquad \omega_k \stackrel{\text{def}}{=} 2\omega_e \sin\frac{\pi k}{N}. \end{aligned} \tag{15}$$

Once λ_n are determined, the displacement and velocity covariances are obtained from the relations:

$$\begin{aligned} &2\kappa_n = \lambda_n + \sigma^2\delta_n^N\,, \qquad \ddot{\xi}_n = 2\lambda_n\,, \\ &\xi_n|_{t=0} = 0\,, \qquad \dot{\xi}_n|_{t=0} = 0; \end{aligned} \tag{16}$$

and centered displacement and velocity dispersions are determined by the covariance values at $n = 0$:

$$\langle \tilde{u}_k^2 \rangle = \xi_0 - \frac{\sigma^2 t^2}{N}\,, \qquad \langle \tilde{v}_k^2 \rangle = \kappa_0 - \frac{\sigma^2}{N}. \tag{17}$$

The dispersions can be conveniently expressed through the function $\lambda(t) \stackrel{\text{def}}{=} \lambda_0 \equiv \lambda_n|_{n=0}$:

$$\langle \tilde{u}_k^2 \rangle = 2\mathcal{I}^2\lambda(t) - \frac{\sigma^2 t^2}{N}\,, \qquad \langle \tilde{v}_k^2 \rangle = \frac{\lambda(t)}{2} + \frac{\sigma^2}{2} - \frac{\sigma^2}{N}, \tag{18}$$

where we use the integral operator

$$\mathcal{I}f(t) \stackrel{\text{def}}{=} \int_0^t f(\tau)\mathrm{d}\tau. \tag{19}$$

According to [3], the $\lambda(t)$ value is proportional to the Lagrangian (the difference of the system's kinetic and potential energies): $\mathcal{L} = \frac{mN}{2}\lambda(t)$. Hereafter $\lambda(t)$ is referred to as the reduced Lagrangian. From formula (15) we obtain

$$\lambda(t) = \frac{\sigma^2}{N}\sum_{k=0}^{N-1}\cos 2\omega_k t\,, \qquad \omega_k \stackrel{\text{def}}{=} 2\omega_e \sin\frac{\pi k}{N}. \tag{20}$$

Substituting expression (20) into relations (18) gives explicit expressions for centered dispersions

$$\langle\tilde{u}_k^2\rangle = \frac{\sigma^2}{N}\sum_{k=1}^{N-1}\frac{\sin^2\omega_k t}{\omega_k^2}\,, \qquad \langle\tilde{v}_k^2\rangle = \frac{\sigma^2}{N}\sum_{k=1}^{N-1}\cos^2\omega_k t, \tag{21}$$

where the frequencies ω_k are defined by formula (20).

IV. THERMAL ECHO

The time dependences for the diffusion and thermal processes are fully determined by the exact analytical formula (21). These relationships are useful for numerical computations, however, they are difficult to use for analytical evaluation because they contain a large number of terms for large N (the most interesting case from a practical point of view). The summands are equivalent and none of them can be neglected. The following identity significantly simplifies the analytical solution [14]

$$\frac{1}{N}\sum_{k=0}^{N-1}\cos\left(z\sin\frac{\pi k}{N}\right) = J_0(z) + 2\sum_{p=1}^{\infty}J_{2pN}(z), \tag{22}$$

where $J_n(z)$ is the Bessel function of the first kind. The identity is proved in the appendix. Using identity (22), formula (20) for $\lambda(t)$ transforms into

$$\lambda(t) = \sigma^2\left(J_0(4\omega_e t) + 2\sum_{p=1}^{\infty}J_{2pN}(4\omega_e t)\right). \tag{23}$$

It may seem that the formula has become more complicated because the sum of a finite number of elementary functions is replaced by an infinite sum of special functions. However, this is not the case. The Bessel functions are virtually zero if the argument value is less (with some margin) than the index value. Therefore, in many practically important cases, formula (23) contains only one or a few important terms. Moreover, the largest Bessel function values for large N occur when the argument values are close to the index value. This is true for the time moments

$$t = pt_*\,, \qquad t_* \stackrel{\text{def}}{=} \frac{N}{2\omega_e}\,; \qquad p = 0, 1, 2, 3, \ldots \tag{24}$$

Then, in the proximity of these time moments, the sum (23) has one main summand, and the rest give only a minor contribution.

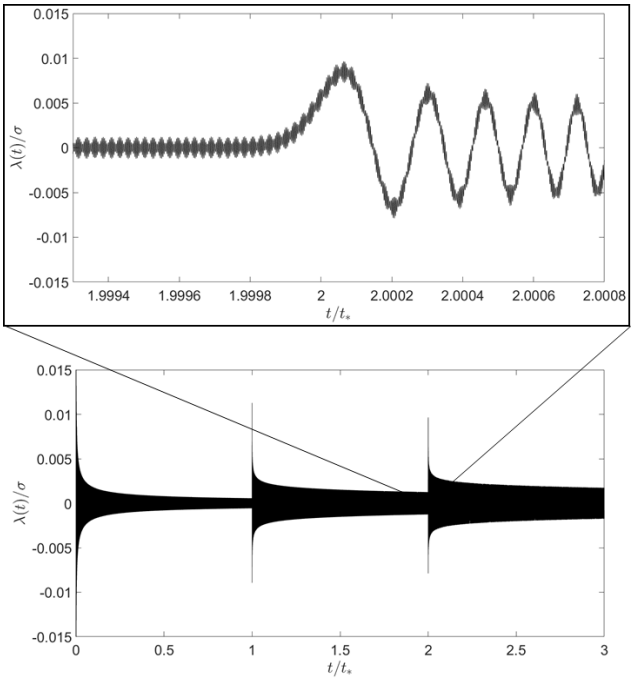

FIG. 1. Time dependence of the reduced Lagrangian for $N = 10^6$. The top figure shows the oscillations near the peak (time resolution increased by 2000 times).

The aforementioned allows us to analyze the diffusion and thermal processes described by formulae (18). The quantity t_* is the quasi-period of these processes. Although the considered processes, strictly speaking, are not periodic, they exhibit certain repeatability with period t_*. As will be shown below, under certain conditions these processes can be assumed to be periodic. The quasi-period has a simple physical meaning:

$$t_* \stackrel{\text{def}}{=} \frac{N}{2\omega_e} = \frac{1}{2}\frac{L}{c_e}, \tag{25}$$

where $L = Na$ is the crystal length, $c_e = \omega_e a$ is the speed of sound, a is the lattice step. Thus, the quasi-period is the time needed for long (sound) waves to pass half-length of the crystal. Over this time, the waves coming from the point source go around the circular (periodic) crystal and meet on its opposite side. At this moment the thermal oscillation amplitude increases rapidly, so-called "thermal echo" occurs. The function $\lambda(t)$ calculated for one million particles is shown in Fig. 1. The abrupt increases in the thermal oscillation amplitude at $t = t_*$ and $t = 2t_*$ are evident. Each of these increases corresponds to one summand in (23), i.e., the respective Bessel function, which is a wave packet with successively decreasing amplitudes. Thus, the physical meaning of transformation (22) is that the summation over the hard-to-observe crystal eigenforms is replaced by the summation over the wave packets perceived as the "thermal echo".

V. INFINITE CRYSTAL

At $N \to \infty$, quasi-period t_* (24) tends to infinity. In this case, for finite t, only the first term is left in formula (23). Then from formulae (18) at the limit of $N \to \infty$ we obtain:

$$\langle \tilde{u}_k^2 \rangle = 2\sigma^2 \mathcal{I}^2 J_0(4\omega_e t)\,, \qquad \langle \tilde{v}_k^2 \rangle = \frac{\sigma^2}{2}\left(1 + J_0(4\omega_e t)\right). \tag{26}$$

The formula for $\langle \tilde{v}_k^2 \rangle = k_B T/m$ was previously obtained in [3]. The displacement dispersion calculation provides

$$\langle \tilde{u}_k^2 \rangle = \frac{\sigma^2}{8\omega_e^2}\,\Phi(4\omega_e t)\,, \qquad \Phi(z) \stackrel{\text{def}}{=} \mathcal{I}^2 J_0(z), \tag{27}$$

where the function $\Phi(z)$ is defined through the Bessel functions J_n and the Struve functions H_n [23]:

$$\Phi(z) = z^2 J_0(z) - z J_1(z) + \frac{\pi}{2}\, z^2 \left(J_1(z) H_0(z) - J_0(z) H_1(z)\right). \tag{28}$$

The function $\Phi(z)$ is plotted in Fig. 2. The function is monotonically increasing, its asymptotics for small and large z are:

$$z \ll 1 \quad \Rightarrow \quad \Phi(z) \simeq \frac{z^2}{2}\,, \qquad\qquad z \gg 1 \quad \Rightarrow \quad \Phi(z) \simeq z. \tag{29}$$

More accurate asymptotics for larger z take the form:

$$z \gg 1 \quad \Rightarrow \quad \Phi(z) \simeq z - J_0(z). \tag{30}$$

Thus, the displacement dispersion of an infinite crystal is a monotonically increasing function of time, which exhibits decaying oscillations near the inclined asymptote. Starting from a certain moment time, the dispersion growth becomes almost linear, coinciding with the asymptote:

$$t \gg t_e \stackrel{\text{def}}{=} \frac{2\pi}{\omega_e}: \qquad \langle \tilde{u}_k^2 \rangle \simeq \frac{\sigma^2}{2\omega_e}\, t. \tag{31}$$

VI. THE FIRST QUASI-PERIOD

Let us consider $t \in [0, t_*]$. In this case, the first two terms in the representation (23) for the reduced Lagrangian must be taken into account

$$\lambda(t) = \sigma^2 \left(J_0(4\omega_e t) + 2J_{2N}(4\omega_e t)\right), \tag{32}$$

which gives the dispersion formulae:

$$\langle \tilde{u}_k^2 \rangle = 2\sigma^2 \mathcal{I}^2 \left(J_0(4\omega_e t) + 2J_{2N}(4\omega_e t)\right) - \frac{\sigma^2 t^2}{N}, \tag{33}$$

$$\langle \tilde{v}_k^2 \rangle = \frac{\sigma^2}{2}\left(1 + J_0(4\omega_e t) + 2J_{2N}(4\omega_e t)\right) - \frac{\sigma^2}{N}. \tag{34}$$

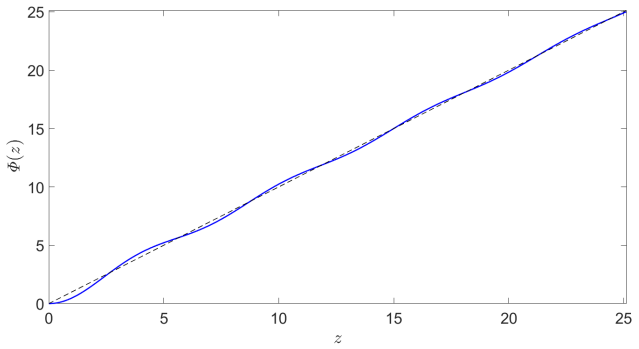

FIG. 2. The function $\Phi(z)$, shows the displacement dispersion growth in an infinite crystal. The dashed line shows the asymptote $\Phi(z) \simeq z$.

Here, unlike in the infinite crystal case, the $1/N$ terms are kept.

Using the formula (34), a simple asymptotic formula can be derived for larger N. Let us use the following approximations: the term $2J_{2N}(4\omega_e t)$ is neglected until approaching the time $t = t_*$, and the iterated integral of the term $J_0(4\omega_e t)$ is replaced by the linear dependence (31). Then we obtain:

$$\langle \tilde{u}_k^2 \rangle \simeq \frac{\sigma^2}{N}\, t\,(t_* - t)\,, \qquad \langle \tilde{v}_k^2 \rangle \simeq \frac{\sigma^2}{2} - \frac{\sigma^2}{N} \tag{35}$$

i.e., displacement dispersion has a quadratic time dependence (inverted parabola), velocity dispersion is a constant. The most significant deviations are at the interval boundaries, but the greater the number of crystal particles, the less noticeable these deviations will be. Fig. 3 shows a comparison [26] of the exact and asymptotic solutions for the displacement dispersion.

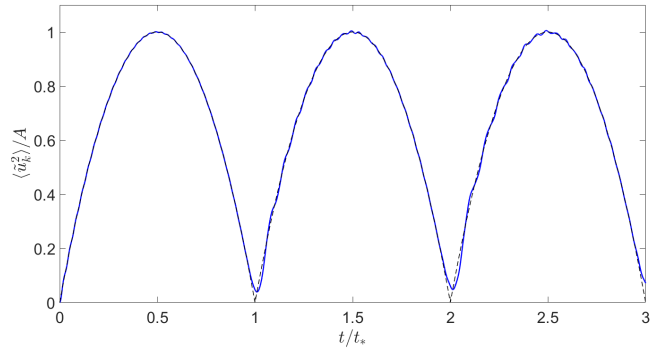

FIG. 3. The centered displacement dispersion dependence on time for $N = 100$ (solid line), the limit at $N \to \infty$ (dashed line), where $A \stackrel{\text{def}}{=} \sigma^2 t_*^2/(4N)$ is the maximum dispersion value at $N \to \infty$.

An unexpected result of the formula (35) is that the displacement dispersion turns zero at $t = t_*$. This indicates that at these time moments the displacements of all particles in the chain turn to zero, i.e., it returns

to the initial state. The required time is large from a microscopic point of view (much more than the atomic oscillation period) but rather short from a macroscopic point of view, i.e., the time it takes the sound to travel half the length of the crystal. Certainly, the result is not exact, because the formula (35) is an approximation. However, it gets more accurate the larger the N is, and for crystals that are long enough, it has a high degree of accuracy. The result resembles the Poincaré recurrence theorem, but this recurrence takes time several orders smaller than that predicted by the Poincaré theorem.

A simple explanation for zero displacements can be provided in terms of eigenforms (normal modes) of crystal oscillations. In the macroscopic (long-wave) approximation, all natural frequencies are divisible by the lowest frequency corresponding to the quasi-period t_*. Thus, the quasi-period t_* contains an integer number of natural periods and thus becomes the crystal's oscillation period. For exact formulae, the higher frequencies are not divisible by the lower frequencies. However, the deviation gets smaller the more atoms the crystal contains, and, consequently, the closer the system is to the macroscopic one. Therefore, the longer the one-dimensional crystal is, the closer the displacements are to zero.

VII. ASYMPTOTICS FOR LARGE N

For large z the following asymptotic representation [27] can be used

$$J_{2pN}(z) \simeq \delta(z - 2pN), \tag{36}$$

where δ is the Dirac delta function, p is a non-negative integer. Therefore

$$\lambda(t) \simeq \frac{\sigma^2}{4\omega_e}\left(\delta(t) + 2\sum_{p=1}^{\infty}\delta(t - pt_*)\right), \tag{37}$$

where we use $\delta(ax) = \delta(x)/a$ for positive a. The representation is periodic, and the quasi-period t_* (25) is the period for function (37). For the quantity t_*, $t_* \sim N$ (25) is true, so the formula (37) corresponds to long periods for large N. In this case, the largest Bessel function values are in the vicinity of time moments pt_*, where $p = 0, 1, 2, 3...$, so the representation (37) can be used as an approximation of expression (32), see Fig. 1.

The formula (37) on the open interval $(0, t_*)$ gives the formula (35) for the dispersions (18) as asymptotically exact representations. At subsequent time intervals of duration t_* the functions are periodically repeated. The result can be represented as

$$\langle\tilde{u}_k^2\rangle \simeq \sum_{p=0}^{\infty} f(t - pt_*)\,, \qquad \langle\tilde{v}_k^2\rangle \simeq \sum_{p=0}^{\infty}\varphi(t - pt_*), \tag{38}$$

where the functions on the closed interval $[0, t_*]$ are

$$\begin{aligned} f(t) &\stackrel{\text{def}}{=} \frac{\sigma^2}{N}\,t\,(t_* - t)\,, \\ \varphi(t) &\stackrel{\text{def}}{=} \frac{\sigma^2}{8\omega_e}\Big(\delta(t) + \delta(t - t_*)\Big) + \frac{\sigma^2}{2} - \frac{\sigma^2}{N} \end{aligned} \tag{39}$$

and are equal to zero outside the specified interval.

According to the representation (38)–(39), after the thermal perturbation the velocity dispersion (and hence the temperature) is almost constant, except for the time moments pt_*, in which localized peaks are observed (the "thermal echo"). It happens because the crystal is finite, so the elastic waves generated by the initial perturbation of each atom interact with each other. This interaction happens when the waves circle the crystal, so the corresponding time t_* is equal to the time it takes the sound wave to travel half-length of the crystal (25). According to the representation (37), all peaks are the same. But according to the exact formula (32), they are different. The height of each successive peak is lower and the width is larger as if the peaks were spreading out, while still retaining the same energy. Based on the Bessel function behavior, each peak is a rapidly arising oscillation, which amplitude then decays in inverse proportion to the square root of time.

The displacement dispersion time function, according to (38)–(39), shows a different behavior (Fig. 3). After the initial thermal impact, the dispersion grows linearly at first, then its growth slows down, and at $t = t_*/2$ it reaches a maximum

$$\langle\tilde{u}_k^2\rangle_{\max} \simeq \frac{\sigma^2 t_*^2}{4N} = \frac{\sigma^2 N}{16\omega_e^2}. \tag{40}$$

According to (40)), the dispersion maximum is proportional to N, so the maximum displacements of the center of mass are proportional to $\sqrt{N}$. After reaching the maximum, the dispersion symmetrically decreases and turns to zero at $t = t_*$. Then the dispersion begins to increase again, and the process repeats itself. This pattern is observable at large macroscopic periods. At small microscopic periods near points $t = pt_*$ transient processes occur. Formulae (38)–(39) define them as a break in displacement time dependence. According to the exact formula (32), the transients are high-frequency oscillatory modes superimposed on the functions (38)–(39).

Note that in formulae (38)–(39) in order to achieve the same accuracy for displacements and velocities we need different N values that vary by orders of magnitude. According to Fig. 3, a good agreement between the exact and asymptotic formulae for the displacement dispersion is obtained for $N = 100$. For the velocity dispersion, however, even at $N = 10^6$ the graphs are quite different from the asymptotic representation[28] (see Fig. 1). This difference occurs because we have to integrate twice in order to get from the velocity dispersion to the displacement dispersion, and the integration has a smoothing effect. The switchback requires a double differentiation, which increases the high-frequency component.

VIII. COMPARISON OF ENSEMBLE AND SPACE AVERAGES

The above-mentioned results for the displacement dispersion apply to the squared displacement mathematical expectation, which is equivalent to averaging over a statistical ensemble. For real systems, this result agrees with the average over a large number of realizations, i.e., experiments with similar initial conditions (statistically identical, but different in terms of individual random values). Generally speaking, the situation for each particular experiment may differ from the one described above. The numerical calculations, that can be verified analytically, show that the spatial average squared displacement in any individual experiment is very different from the average statistical result given by formulae (38)–(39). This phenomenon is shown [29] in Fig. 4, showing the time dependences of

$$\{\tilde{u}_k^2\} \stackrel{\text{def}}{=} \frac{1}{N}\sum_{k=1}^{N}\tilde{u}_k^2 = \frac{1}{N}\sum_{k=1}^{N}(u_k-\overline{u})^2. \qquad (41)$$

Here the curly brackets denote averaging over space (or over particles, the same thing in this case). Hereafter, for the sake of brevity, we denote the value $\{\tilde{u}_k^2\}$ as the mean squared displacement. The time dependences of the mean squared displacements shown in Fig. 4 were obtained from the numerical solution of the initial value problem (1)–(3) for various realizations of random initial conditions. Unlike the dispersion $\langle\tilde{u}_k^2\rangle$, which is a deterministic quantity, the mean squared displacement $\{\tilde{u}_k^2\}$ is a stochastic quantity, and for different realizations, different graphs are obtained. The function $\{\tilde{u}_k^2\}(t)$, as well as $\langle\tilde{u}_k^2\rangle(t)$, approaches zero periodically at $t = pt_*$, and almost repeats in each new quasi-period. However, between zero points, the time dependences in different experiments vary in shape, often significantly distinct from the parabolic one. The maximum values can vary dramatically (by a factor of several times), and within a single quasi-period there can be several maxima.

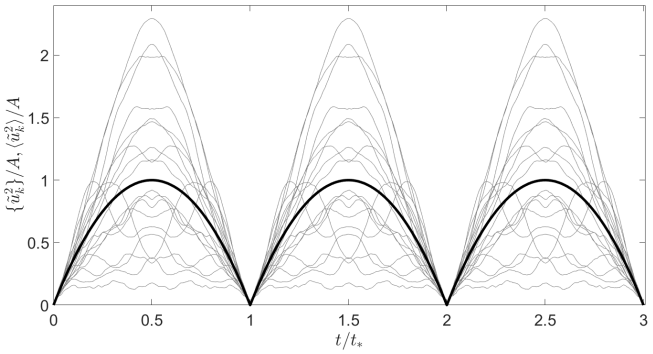

FIG. 4. Spatial mean squared displacement $\{\tilde{u}_k^2\}$ for different realizations at $N = 1000$ (thin lines), displacement dispersion $\langle\tilde{u}_k^2\rangle$ (bold line), scale multiplier $A \stackrel{\text{def}}{=} \sigma^2 t_*^2/(4N)$.

The function $\langle\tilde{u}_k^2\rangle(t)$ is the mathematical expectation of the functions $\{\tilde{u}_k^2\}(t)$, i.e., is the limit of averages over random initial condition realizations. However, the functions $\langle\tilde{u}_k^2\rangle(t)$ do not tend to $\{\tilde{u}_k^2\}(t)$ as the number of particles increases. Even for very large N, the mean squared displacement $\{\tilde{u}_k^2\}$ remains a stochastic variable. Thus, the spatial average and the ensemble average are essentially different for the squared displacements. Note that the case is different for velocities: as N increases the mean squared velocity $\{\tilde{v}_k^2\}$ tends to a deterministic value $\langle\tilde{v}_k^2\rangle$, i.e., the velocity dispersion proportional to the crystal kinetic temperature. This is the fundamental difference between thermal and diffusion processes. The results of analogous calculations are given in the book [25]

IX. CONCLUSION

This paper considers the processes occurring in a periodic (circular) one-dimensional crystal under instantaneous spatially uniform thermal perturbation. We obtained exact time dependences for thermal and diffusion characteristics, such as dispersions of particle velocities and displacements. The most notable formulae are: (21) are the exact formulae for centered velocity and displacement dispersions, convenient for numerical calculations; (22) is the shift from the summation over eigenforms to the summation over wave packets; (18), (23) are the alternative formulae for velocity and displacement dispersions that are convenient for analytic analysis; (27)–(28) are the time dependence of displacement dispersion for an infinite crystal; (38)–(39) are the asymptotic expressions for velocity and displacement dispersions for large N.

In the infinite crystals, thermal characteristics are represented by damped oscillations described by the Bessel function, following the results obtained earlier [3]. Diffusion characteristics show unlimited growth close to linear (Fig. 2).

For a finite crystal, the oscillations of the thermal characteristics resume after a time it takes the sound wave to travel the half-length of the crystal (Fig. 1). Such kinetic temperature peaks can be understood as "thermal echo" caused by the elastic waves from the excited particle traveling around the crystal and meeting on the opposite side from their origin point. As time passes, the successive peaks lose amplitude, but increase in width, preserving the energy they contain. Thus, the crystal undergoes fast periodic transient processes.

The diffusion characteristics, besides similar fast processes, also demonstrate a slow process, namely the dispersion growth up to a value proportional to the number of particles and further displacement dispersion reduction to zero at the time of the next temperature burst (Fig. 3). Thus, the crystal returns to a state similar to the initial state after half the time it takes for the sound wave to travel through the crystal, a period insignificant in macroscopic terms. The more particles are in the crystal, the stronger is the recurrence phenomenon and the closer the dispersion behavior is to the parabolic one.

The space mean squared displacement differs from the statistical average across realizations: the first quantity is stochastic (for any number of particles), the second one is deterministic (see Fig. 4).

Thus, thermal and diffusion processes in a finite crystal are much more complex than in an infinite one. In turn, diffusion processes in the finite crystal are more complex than thermal processes. They include fast and slow processes, the average across the crystal remains stochastic even when the number of particles is huge. The most important discovered phenomena are (i) the thermal echo (periodic temperature peaks), (ii) the periodic return of system particles to their initial position, and (iii) the stochastic nature of spatial mean squared displacement.

The described results can be observed when an ultrashort laser impacts a nanostructure. They can also provide a basis for a more complex process description, such as heat and mass transfer in defectless crystals and nanostructures.

ACKNOWLEDGMENTS

The authors would like to express their sincere gratitude to D.A. Indeitsev and V.A. Kuzkin for their time and useful discussions.

The research is partially funded by the Ministry of Science and Higher Education of the Russian Federation as part of World-class Research Center program: Advanced Digital Technologies (contract No. 075-15-2020-934 dated 17.11.2020)

APPENDIXES

Appendix A: Proof of identity (22)

Let us use the formula [24]:

$$\cos(z\sin\theta) = \sum_{p=-\infty}^{\infty} J_{2p}(z)\cos(2p\,\theta), \tag{A1}$$

where $J_{2p}(t)$ is the Bessel function of the first kind. Substituting $\theta = \pi k/N$, where $k = 0, 1, ..., N-1$, and summing over k, we obtain:

$$\frac{1}{N}\sum_{k=0}^{N-1}\cos\left(z\sin\frac{\pi k}{N}\right) = \sum_{p=-\infty}^{\infty} J_{2p}(z)S_N(p), \tag{A2}$$

where

$$S_N(p) \stackrel{\text{def}}{=} \frac{1}{N}\sum_{k=0}^{N-1}\cos\left(p\,\frac{2\pi k}{N}\right). \tag{A3}$$

The sum of multiple angle cosines can be calculated through the sum of exponents, which, in turn, is calculated as the geometric progression sum:

$$\sum_{k=0}^{N-1}\cos k\phi = \mathrm{Re}\sum_{k=0}^{N-1} e^{ik\phi} = \mathrm{Re}\left(\frac{e^{iN\phi}-1}{e^{i\phi}-1}\right). \tag{A4}$$

Calculating the real part of (A4) gives the following representation:

$$\sum_{k=0}^{N-1}\cos k\phi = \frac{1}{2}\sin(N\phi)\,\mathrm{ctg}\,\frac{\phi}{2} + \sin^2\frac{N\phi}{2}, \tag{A5}$$

whence we find

$$S_N(p) = \frac{\sin(2\pi p)}{2N}\,\mathrm{ctg}\frac{\pi p}{N} + \frac{\sin^2(\pi p)}{N}. \tag{A6}$$

Analysis of the obtained expression shows that for p divisible by N it is equal to one and for all other integer p it is equal to zero. To put it otherwise, $S_N(p) = \delta_p^N$. Then for the formula (A2) we finally get:

$$\frac{1}{N}\sum_{k=0}^{N-1}\cos\left(z\sin\frac{\pi k}{N}\right) = \sum_{p=-\infty}^{\infty} J_{2pN}(z) = J_0(z) + 2\sum_{p=1}^{\infty} J_{2pN}(z), \tag{A7}$$

where we use that $J_n(x) = J_{-n}(x)$ for all integer n.

[1] Rieder Z., Lebowitz J. L. and Lieb, E. Properties of a harmonic crystal in a stationary nonequilibrium state. J. Math. Phys. 1967. vol. 8, pp. 1073–1078.

[2] Dhar A. Heat Transport in low-dimensional systems. Advanced in Physics. 2008. Vol. 57, No. 5, pp. 457–537.

[3] Krivtsov A. M. Energy Oscillations in a One-Dimensional Crystal. Doklady Physics. 2014, Vol. 59, No. 9, pp. 427-430.

[4] Krivtsov A. M. Heat transfer in infinite harmonic one dimensional crystals. Doklady Physics. 2015, Vol. 60, No.

9, pp. 407-411.
[5] Thermal transport in low dimensions: from statistical physics to nanoscale heat transfer. Edited by S. Lepri. Lecture notes in physics, volume 921. Springer International Publishing, Switzerland. 2016, 418 p.
[6] V.A. Kuzkin, A.M. Krivtsov. Fast and slow thermal processes in harmonic scalar lattices. Journal of Physics: Condensed Matter, 2017, Vol.29, No.50
[7] Poletkin K. V., Gurzadyan G. G., Shang J., Kulish V. Ultrafast heat transfer on nanoscale in thin gold films. Applied Physics B. 2012. 107 (01), pp. 137–143.
[8] Cartlidge E. European xfel to shine as brightest, fastest x-ray source. Science. 2016. Vol. 354, no. 6308, pp. 22-23.
[9] Albertazzi B., Ozaki N., Zhakhovsky V. et al. Dynamic fracture of tantalum under extreme tensile stress. Science Advances. 2017. Vol. 3, no. 6.
[10] Krivtsov A. M., Morozov N. F. On Mechanical Characteristics of Nanocrystals. Physics of the Solid State. 2002. Volume 44, Issue 12, pp 2260-2265.
[11] Goldstein R.V., Morozov N.F. Mechanics of deformation and fracture of nanomaterials and nanotechnology. Physical Mesomechanics. 2007. Vol 10, p. 5-6.
[12] Levin V.A., Levitas V.I., Lokhin V.V., Zingerman K.M., Sayakhova L.F., Freiman E.I. Solid-state stress-induced phase transitions in a material with nanodimensional inhomogeneities: Model and computational experiment. Doklady Physics. 2010. Vol. 55, No. 10, pp. 507-511.
[13] Indeitsev D.A., Loboda O.S., Morozov N.F., Skubov D.Yu., Shtukin L.V. Self-oscillating mode of a nanoresonator. Physical Mesomechanics. 2016. Vol.19. No 5. pp. 23-28.
[14] Murachev, A., Krivtsov, A. M., Tsvetkov, D. (2018). Thermal echo in a finite one-dimensional harmonic crystal. Journal of Physics: Condensed Matter
[15] Florencio J., Lee M. H. Exact time evolution of a classical harmonic-oscillator chain. Phys. Rev. A, 1985. Vol. 31, 3231 p.
[16] Krivtsov A. M. Deformation and fracture of solids with microstructure. Moscow, Fizmatlit. 2007. 304 p. (In Russian).
[17] Gendelman O. V., Savin A. V. Normal heat conductivity in chains capable of dissociation. Europhys. Lett. 2014. Vol. 106, p. 34004.
[18] Savin A. V., Kosevich Y. A. Thermal conductivity of molecular chains with asymmetric potentials of pair interactions. Phys. Rev. E. 2014. Vol. 89, 032102.
[19] Berinskii I. E., Slepyan L. I. How a dissimilar-chain system is splitting. Quasi-static, subsonic and supersonic regimes. 2017. arXiv:1704.00046v2.
[20] Ashcroft N. W. and Mermin N.D. Solid State Physics. Holt, Rinehart and Winston. 1976. 847 p.
[21] Krivtsov A. M. On unsteady heat conduction in a harmonic crystal. 2015. ArXiv:1509.02506.
[22] Krivtsov A. M. Dynamics of thermal processes in one-dimensional harmonic crystals. Questions of mathematical physics and applied mathematics. - Proceedings of the seminar timed to the 75th anniversary of prof. E.A. Tropp. 30 September 2015. – SPb.: A.F. Ioffe Physico-Technical Institute , 2016. pp. 63-81.
[23] Yanke E., Emde F., Lesh F. Special functions: the formulae, graphs, tables. Science. 1964, Moscow, 344 p.
[24] Abramowitz M. and Stegun I. A. Handbook of Mathematical Functions With Formulas, Graphs, and Mathematical Tables. New York: Dover. 1979. 1046 p.
[25] Hoover, W. G., Hoover, C. G. (2018). Microscopic and Macroscopic Simulation Techniques: Kharagpur Lectures. World Scintific.
[26] The graphs shown in Fig. 3, are obtained as a result of integration in the formula (33), however, for numerical calculation, it is more convenient to use the formula (21).
[27] This representation means that the Bessel function tends to the delta function with the corresponding axis scale change. Formally this can be expressed as $AJ_n(A(z-n)+n) \to \delta(z-n)$ at $A \to \infty$, where the limit is understood in a weak (generalized) form. For the Bessel function integrals, required to determine the displacement dispersion, this limit and the corresponding asymptotics are considered in a traditional form.
[28] According to formula (18), the velocity dispersion is linearly related to the reduced Lagrangian (23), o the graph in Fig. 1 represents the velocity dispersion time dependence.
[29] The interactive graphs are available at tm.spbstu.ru/uu